



Research article

Promising brain biodistribution of insulin via intranasal dry powder for nose-to-brain delivery

Cynthia Marisca Muntu^{a,b}, Christina Avanti^b, Hayun^c, Silvia Surini^{a,*}^a Laboratory of Pharmaceutics and Pharmaceutical Technology, Faculty of Pharmacy, Universitas Indonesia, Depok 16424, West Java, Indonesia^b Department of Pharmaceutics, Faculty of Pharmacy, Universitas Surabaya, Surabaya 60293, East Java, Indonesia^c Laboratory of Pharmaceutical and Medicinal Chemistry, Faculty of Pharmacy, Universitas Indonesia, Depok 16424, West Java, Indonesia

ARTICLE INFO

Keywords:

Biodistribution
Dry powder
Histopathology
Insulin
Mucoadhesive
Nose-to-brain
Permeation
Release

ABSTRACT

Nose-to-brain delivery (NTBD) offering potential benefits for treating Alzheimer's disease. In previous research, insulin dry powder (IDP) formulation for NTBD was developed, exhibiting favorable stability. This study aims to conduct *in vitro* and *ex vivo* assessment of release, permeation, mucoadhesion and histopathology, as well as an *in vivo* biodistribution study to produce IDP for NTBD and evaluate brain biodistribution. Spray-freeze-dried IDP formulations with varying weight ratios of trehalose-to-inulin were produced and analyzed. The release study was carried out in PBS with a pH of 5.8 stirred at 50 rpm and maintained at 37 °C ± 0.5 °C. Goat nasal mucosa was used for *ex vivo* permeation and mucoadhesion testing under similar conditions. An *ex vivo* histopathological examination and an *in vivo* study using enzyme-linked immunosorbent assay, were also performed. The IDP dissolution study demonstrated complete release of all IDPs within 120 min. The permeation study indicated that steady-state conditions were observed between 30 and 240 min. The mucoadhesion study unveiled that IDP F5 exhibited the fastest mucoadhesion time and the least force required within the fastest time of 43.60 ± 2.57 s. The histopathological study confirmed that none of the tested IDPs induced irritation in the nasal mucosa. Furthermore, the biodistribution study demonstrated the absence of detectable insulin in the plasma, while IDP F3 exhibited the highest deposited concentration of insulin within both the olfactory bulb and the whole brain. The extensive evaluation of the IDP formulations through *in vitro*, *ex vivo*, and *in vivo* studies implies their strength non-invasive NTBD. IDP F3, with a 1:1 wt ratio of trehalose to inulin, exhibited favorable brain biodistribution outcomes and was recommended for further investigation and development in the context of NTBD.

1. Introduction

Nose-to-brain delivery (NTBD) is a promising non-invasive approach for directly administering therapeutic agents to the brain through the nasal cavity [1]. Olfactory neurons in this cavity serve not only for the sense of smell but also facilitate the rapid transport of drugs across the cribriform plate, bypassing the blood-brain barrier (BBB) [2]. This unique advantage over systemic routes, such as oral or injection [3], holds great potential for enhancing the efficacy of treatments for neurological disorders including Alzheimer's

* Corresponding author. Laboratory of Pharmaceutics and Pharmaceutical Technology, Faculty of Pharmacy, Universitas Indonesia, Depok, West Java, 16424, Indonesia.

E-mail addresses: cynthia_muntu@staff.ubaya.ac.id (C.M. Muntu), c_avanti@staff.ubaya.ac.id (C. Avanti), hayun.ms06@gmail.com (Hayun), silvia@farmasi.ui.ac.id (S. Surini).

<https://doi.org/10.1016/j.heliyon.2024.e33657>

Received 21 October 2023; Received in revised form 24 June 2024; Accepted 25 June 2024

Available online 26 June 2024

2405-8440/© 2024 The Authors. Published by Elsevier Ltd. This is an open access article under the CC BY-NC license (<http://creativecommons.org/licenses/by-nc/4.0/>).

disease (AD) [4].

With approximately 36 million individuals afflicted worldwide, AD represents a growing global health challenge. Specifically, 17 million of those individuals reside in Asia, while over 4 million elderly individuals in the United States currently affected by AD. This number is projected to increase nearly fourfold by the year 2050 [5]. Even younger individuals are now being impacted by AD. Patients with typical AD who are also younger frequently experience delayed diagnosis [6]. Currently, treating AD involves a comprehensive symptom management strategy to preserve the quality of life, alleviate the impact of the condition, and reduce long-term clinical decline. Effective extended pharmacotherapy of FDA-approved medications for Alzheimer's disease typically starts with a single-agent treatment involving a cholinesterase inhibitor (ChEI) donepezil, galantamine, and rivastigmine. Moreover, the treatment of AD eventually progressed to a supplementary combination therapy involving both a ChEI and memantine [7].

Furthermore, based on recent research, AD can be addressed using insulin. This is due to the association of insulin with its role in enhancing the expression and translocation of brain glucose transporter-4 (GLUT-4), which further contributes to glucose uptake by brain cells [8,9]. In recent research, insulin has been reported to influence learning and memory functions [10]. The research in this field has advanced clinical trials. Administering liquid insulin at a dosage of 20 IU through the intravenous route in AD patients yielded improvements in cognition. Nonetheless, this administration led to a significant and substantial reduction in blood glucose levels [11]. Consequently, further studies on insulin use for AD patients have shifted focus to the intranasal route, utilizing nose-to-brain delivery (NTBD). Administering 20 IU of liquid insulin via the intranasal route yielded favorable outcomes without inducing hypoglycemic side effects [12,13]. All of the mentioned research used a product available on the market, which is diabetic-purpose insulin, insulin solution which is used intranasally in AD patients [11–13]. Additionally, another study explored intranasal insulin formulation in the form of a nanogel, which was tested using an animal model [14]. The use of the intranasal route and this delivery aim to enhance insulin accumulation in the brain while minimizing the occurrence of hypoglycemic side effects.

The clinical testing research of insulin usage in AD patients used an insulin liquid product, yet this can disrupt insulin stability, particularly during long-term storage. Currently, liquid insulin available on the market is stored under cold chain distribution conditions. This condition requires costly and complex handling procedures [15]. Nevertheless, inadequate adherence to proper handling or disruptions in the process can reduce insulin's stability, potentially diminishing its efficacy [16]. Moreover, its physicochemical stability is compromised in liquid formulations, resulting in a short shelf life of approximately one month after being opened [17].

In a previous study, insulin dry powder (IDP) for intranasal purpose has been studied, and the results demonstrated improved physicochemical stability of insulin [18,19]. In this study, to ensure the safety and efficacy of IDP, further research on the IDP encompassing *in vitro*, *ex vivo*, and *in vivo* studies has been conducted. IDPs were produced using the same method as the previous study [18,19]. The obtained IDP was assessed in regard to its insulin content, particle size and shape. Furthermore, *in vitro* release and mucoadhesion studies were conducted using goat nasal mucosa to provide important insights into the behavior and performance of the IDP formulations. *Ex vivo* studies on permeation, mucoadhesion, and histopathology were subsequently performed to assess the interaction of the produced IDPs with nasal tissues, providing a more realistic representation of the nasal environment. Moreover, an *in vivo* biodistribution study was also carried out to investigate the transport and delivery of insulin to the olfactory region and brain after intranasal administration. The acquired data are crucial for understanding the distribution of insulin in the targeted area. Therefore, this study aimed to produce IDP for NTBD and evaluate brain biodistribution.

2. Materials and methods

2.1. Materials

The five different IDP formulations were prepared from various materials. The active pharmaceutical ingredient (API), which is insulin human acidic fibroblast (AF), were procured from Sigma Aldrich, St. Louis, MO, USA. The excipients, including trehalose and HPMC E5, were sourced from Meihua Holding Group Co., Ltd. (Langfang, Hebei, China), while inulin and poloxamer 188, were sourced from Beneo GmbH (Mannheim, Germany). Water for injection were procured from Ikapharmindo Putramas, Jakarta, Indonesia, was used for IDP characterization. Additionally, Whatman nylon membrane filters with a pore size of 0.2 μm from GE Healthcare Life Sciences, Buckinghamshire, UK were employed for filtration purposes. To conduct the analytical procedures, Toluene, KH_2PO_4 , NaOH, HCl (pro analysis), high-performance liquid chromatography (HPLC) grade acetonitrile and methanol, as well as

Table 1
Formulation of IDP.

Material	Formula				
	F1	F2	F3	F4	F5
Human recombinant insulin (IU)	50	50	50	50	50
HPMC E5 (g)	0.01	0.01	0.01	0.01	0.01
Poloxamer 188 (g)	0.01	0.01	0.01	0.01	0.01
Trehalose (g)	1.44	1.15	0.86	0.58	0.29
Inulin (g)	0.29	0.58	0.86	1.15	1.44
HCl 0.1 N (mL)	0.5	0.5	0.5	0.5	0.5
NaOH 0.1 N (mL)	1	1	1	1	1
Aqua destilata (mL)	15	15	15	15	15

spectroscopy grade trifluoroacetic acid, were procured from Merck, Darmstadt, Germany. For *in vitro* and *ex vivo* studies, goat nasal mucosa samples were obtained from the regional animal slaughterhouse company, located in Pegirian, Surabaya. Neutral buffered formalin was purchased from Sumber Ilmiah Persada, Surabaya, while hematoxylin-eosin (HE) and isopropyl alcohol were bought from Leica Biosystem, Richmond, Virginia, United States. Wistar strain rats for the *in vivo* biodistribution study were sourced from UD Mandiri, Surabaya. The human insulin ELISA kit was procured from Calbiotech, California. Protease inhibitor tablets were obtained from Thermo Fisher Scientific, Illinois, and sodium thiopental was purchased from Bernofarm, Sidoarjo, Indonesia.

2.2. Methods

2.2.1. Preparation of insulin dry powder (IDP)

During IDP preparation through the spray-freeze drying (SFD) process, five variations of the IDP formula as listed in Table 1 were used with different weight ratios of trehalose and inulin as stabilizers. The variations, IDP F1 to F5, were formulated with trehalose and inulin at weight ratios of 5:1, 2:1, 1:1, 1:2, and 1:5, respectively. The excipients were weighed and dissolved in water, while insulin was weighed and dissolved in HCl. The resulting solution was mixed and adjusted to a pH of 5.8 before being subjected to the SFD process using liquid nitrogen. Subsequently, the frozen droplets were freeze-dried for approximately 50 h to obtain IDP [18].

2.2.2. Characterization of IDP

2.2.2.1. Particle size. Particle size distribution testing was carried out using an LS Particle Size Analyzer (Beckman Coulter, Washington D. C, USA) based on the principle of Laser Light Scattering. The powder sample was dispersed in toluene before testing to obtain the particle size distribution profile and statistical arithmetic volume diameter data tabulation.

2.2.2.2. Particle shape and surface. The shape and surface of IDP particles were observed at 250 times magnification under a Scanning Electron Microscope (SEM) (Ametek Edax, Berwyn, Pennsylvania, USA) after coating the sample with palladium-gold for 90 s using a sputter coater.

2.2.2.3. Insulin content. The insulin level in the dry powder was analyzed using reversed-phase (RP) High-Performance Liquid Chromatography (HPLC) with Capcell Pak C18 column. The mobile phase consisted of a mix of 0.1 % trifluoroacetic acid in water and acetonitrile in a 70:30 ratio with a flow rate of 1.0 mL/min, and an injection volume of 20 μ L. Furthermore, the process of detection was conducted using a UV detector at a wavelength of 276 nm. The analysis method underwent validation and system suitability testing, and the results met all requirements [18].

2.2.3. *In vitro* release study

A modified dissolution procedure was used to test the dissolution and release of insulin from the powder. Powder samples (0.26 mg insulin equivalent) were placed in a dialysis bag and suspended at a specific height in a beaker containing 80 mL of PBS media at a pH of 5.8, maintained at $37 \text{ }^\circ\text{C} \pm 0.5 \text{ }^\circ\text{C}$ to simulate nasal fluids. The PBS medium was stirred using a magnetic stirrer at 50 rpm to ensure sample homogeneity, following the recommendations of Surini et al. (2018) [20] and Trotta et al. (2018) [21]. Samples of 1 mL were collected at 15, 30, 45, 60, 75, 90, 120, 180, and 240-min intervals. The insulin level in the sample was determined using HPLC as described in the insulin content determination procedure. The insulin release studies were performed in triplicate, and mean values were plotted against time.

Since the insulin release kinetics follow the first order, the percentage of the remaining amount of insulin on a logarithmic scale was plotted against time. The dissolution rate constant could be obtained from the slope value. Other dissolution parameters, such as the dissolution efficiency value and area under the curve (AUC), were also determined.

2.2.4. *Ex vivo* permeation study

The permeation study was conducted using nasal mucosa isolated from the nose of goats opened by a longitudinal incision to obtain the septum. The nasal mucosa was carefully removed from the cartilage bone and immediately dipped into PBS media (pH 5.8), frozen in liquid nitrogen, and stored at $-20 \text{ }^\circ\text{C}$ until used. This was placed in the receptor compartment of the Franz diffusion cell, then stabilized in PBS media (pH 5.8) in both the donor and receptor compartments. Subsequently, the receptor compartment was filled with 70 mL of PBS media (pH 5.8) and maintained at $37 \pm 0.5 \text{ }^\circ\text{C}$.

Ex vivo permeation study of insulin was conducted using the Franz diffusion cell. Approximately 0.5 g of the powder was dispersed onto the nasal mucosa membrane of goats measuring 7.065 cm^2 , which was then placed between the donor and receptor compartments with the mucosal side directly in contact with the receptor medium. The PBS media were stirred with a magnetic stirrer at 50 rpm to ensure sample homogeneity. Samples of 1 mL from the receptor compartment were drawn at regular time intervals, filtered through a $0.45 \text{ }\mu\text{m}$ membrane filter paper, and analyzed using the HPLC method as described in the insulin content determination procedure. Sampling points were selected at 15, 30, 60, 90, 120, 180, 240, 300, and 360 min.

The cumulative amount of insulin permeated through the nasal mucosa was plotted against time, and the steady-state permeation flux was determined from the slope values. The data were expressed as the mean values \pm SD in three replications of observations [22, 23].

2.2.5. *In vitro* mucoadhesion study

To evaluate *in vitro* mucoadhesion strength and measure mucoadhesive ability, a modified balance instrument was employed. Goat nasal mucosa tissue fixed in 10 % formalin buffer was used for this experiment by placing it onto the tissue holder (plate). The insulin powder was compressed into the plate and then attached to the goat nasal mucosa surface for a sufficient contact time of 1 min. Subsequently, the nasal mucosa tissue was placed on the mucoadhesive measuring instrument. The tensile strength test was initiated with the smallest weight, and additional force was applied until the insulin plate began to detach from the goat nasal mucosa within the shortest time possible. This procedure measured the bioadhesive strength in milligrams.

2.2.6. *Ex vivo* mucoadhesion study

The *ex vivo* mucoadhesion time test was conducted using goat nasal mucosa that had been fixed in 10 % neutral buffered formalin and PBS with pH 5.8. The previously prepared mucosa was placed on a tissue holder disk, and IDP was compressed and attached to its surface. The disk, attached to the mucosa and sample, was then placed in a beaker containing 150 mL of phosphate buffer (pH 5.8). Stirring was maintained at a speed of 50 rpm, and the temperature was kept at 37 °C [24]. The adhesion of IDP was observed, and the time required for the insulin powder compressed plate to detach from the goat nasal mucosa was quantitatively measured.

2.2.7. *Ex vivo* histopathology study

The IDP formulation irritation test with goat nasal mucosa was used to observe the impact of the sample on the morphology of the mucosa [25,26]. The nasal mucosa was obtained in the same manner as in the permeation test and fixed in 10 % neutral buffered formalin. Subsequently, it was sectioned with a microtome and stained with hematoxylin-eosin (HE). This test involved several groups: Group 1 was given a PBS solution (negative control), while Group 2 received a 1 % isopropyl alcohol solution (positive control) in a volume of 1 mL and was allowed to stand for 30 min. Nasal mucosa in groups 3–7 were administered with IDP formulation using the same preparation method as the negative and positive controls, then the morphology was observed under an optical microscope [25]. After staining with HE, the epithelial lesion score was determined by following specific criteria, namely, a score of 0 for normal epithelium, 1 for cilia loss, 2 for erosion occurring in the upper part of the epithelium while the lower part remained intact, and 3 for complete erosion of the epithelium [27].

2.2.8. *In vivo* biodistribution study

The biodistribution study of IDP in rats was conducted following ethical guidelines approved by the Institutional Ethical Committee of the University of Surabaya (Number 227/KE/XII/2021). Male Wistar rats weighing 180–200 g were used [14] while being housed under controlled environmental conditions with a temperature of 22–24 °C and relative humidity of 50–60 %. During the acclimatization period, they had ad libitum access to water and food [28]. The test animals were divided into six treatment groups: group 1 given blank samples and groups 2–6 with intranasal IDP treatment groups administered with an insulin dose of 1 IU/kg body weight. The blank samples, which consisted of PBS pH 5.8, were observed as the normal control for each intranasal administration time point. Sampling was performed at five points, namely 0, 15, 60, 90, and 120 min. Each time point consisted of three rats ($n = 3$), leading to a total of 90 rats across all treatment groups and time points.

The rats were anesthetized with intraperitoneal (i.p) injection of Thiopental Na (50 mg/kg) and positioned in a supine position. Supplementary doses of Thiopental Na (12.5 mg/kg) were administered hourly to sustain anesthesia. The rats were handled using the left hand, and a specific amount of IDP (1 IU/kg body weight) and negative control was administered intranasally through an insufflator [23].

At each sampling time point, blood samples of 0.2 mL was drawn from the right jugular vein. Subsequently, the rats were decapitated swiftly, and the whole brain was extracted, followed by rinsing with PBS (pH 7.4). After eliminating excess moisture, the brain samples were divided into two parts: the olfactory bulb and the remaining fragments, while their weights were recorded. The brain samples were homogenized in a solution of four times the initial volume of PBS (pH 7.4) containing 0.001 % methylcellulose and 2 mM PCMB, an insulin degradation enzyme inhibitor, using a glass tissue homogenizer. Both blood and brain samples underwent centrifugation at 4 °C and 5400×g for 15 min. Afterward, plasma and supernatant samples were collected for homogenization in order to determine the concentration of deposited insulin in the tissue or plasma. This determination was conducted utilizing an enzyme-linked immunosorbent assay (ELISA) with a kit specifically designed for human insulin. The absorbance was measured at 450 nm with a FLUOstar omega ELISA microplate reader (BMG LABTECH, Offenburg, Germany). The obtained absorbance values were interpolated against the standard curve equation to calculate the deposited insulin concentration [28].

3. Result and discussion

IDP for NTBD has emerged as a promising approach for treating neurodegenerative diseases such as AD. In this study, IDP was characterized in terms of particle size, shape, surface, and insulin content, while its *in vitro* release and *ex vivo* permeation properties were evaluated. Additionally, mucoadhesion and histopathology studies were conducted to investigate all possible irritation or damage to the nasal mucosa caused by IDP. The results provided important insights into the physicochemical and biopharmaceutical properties of IDP and its potential as a nasal drug delivery system for brain-specific targeting.

3.1. Characteristics of IDP

The aim of characterizing IDP was to ensure its compliance with NTBD powder criteria. The criteria include fine powder with

spherical particle shapes and diameters ranging from 15 to 25 μm . The assessment process covered physical appearance, particle size, particle shape and surface characteristics, and insulin content.

3.1.1. Physical appearance

The IDPs generated from various formulations exhibited the physical appearance characteristics of a fine white powder and were odorless. These characteristics were consistent with those found in the previous study that used the same method and process variables. The characteristics were acquired from the applied SFD method, which involved atomization through a nozzle in the initial stage [18]. The atomization process included the creation of contact between droplets and liquid nitrogen, yielding frozen droplets similar to snow. Subsequently, freeze-drying was performed to produce the fine white powder. All materials used in the formulation were odorless, leading to an odorless powder. This aligned with previous investigations employing the SFD method to produce microparticles or dry powder [18,29].

3.1.2. Particle size

The data obtained from the observation of particle size distribution in surface volume diameter (dvs) were presented in the form of a histogram. Fig. 1 shows the particle size distribution of IDP formulations F1 (A), F2 (B), F3 (C), F4 (D), and F5 (E), each with varying weight ratios of trehalose to inulin: 5:1, 2:1, 1:1, 1:2, and 1:5, respectively. Fig. 1 and Table 2 show that IDP F4 exhibited the smallest mean particle size with a dvs of 18.53 μm , while F2 had the largest mean particle size with a dvs of 23.60 μm . The statistically significant difference in mean particle size between IDP F2 and F4 ($p < 0.05$) is attributed to variations in the b/b ratio of the excipients within the IDP formulations. Specifically, F2 contains trehalose with a weight ratio of 2:1 to inulin, while F4 features a reversed weight ratio of 1:2. These findings are in line with earlier investigations involving chitosan-based insulin microparticles designed for oral delivery. Consistently, the study found that using the highest amount of chitosan resulted in the largest dvs [30]. The significant differences in the dvs parameter might be related to different moisture contents in the dry powder. A higher moisture content would initiate particle aggregation. This was also consistent with the results of the moisture content in IDP, which was lowest in F4 and had

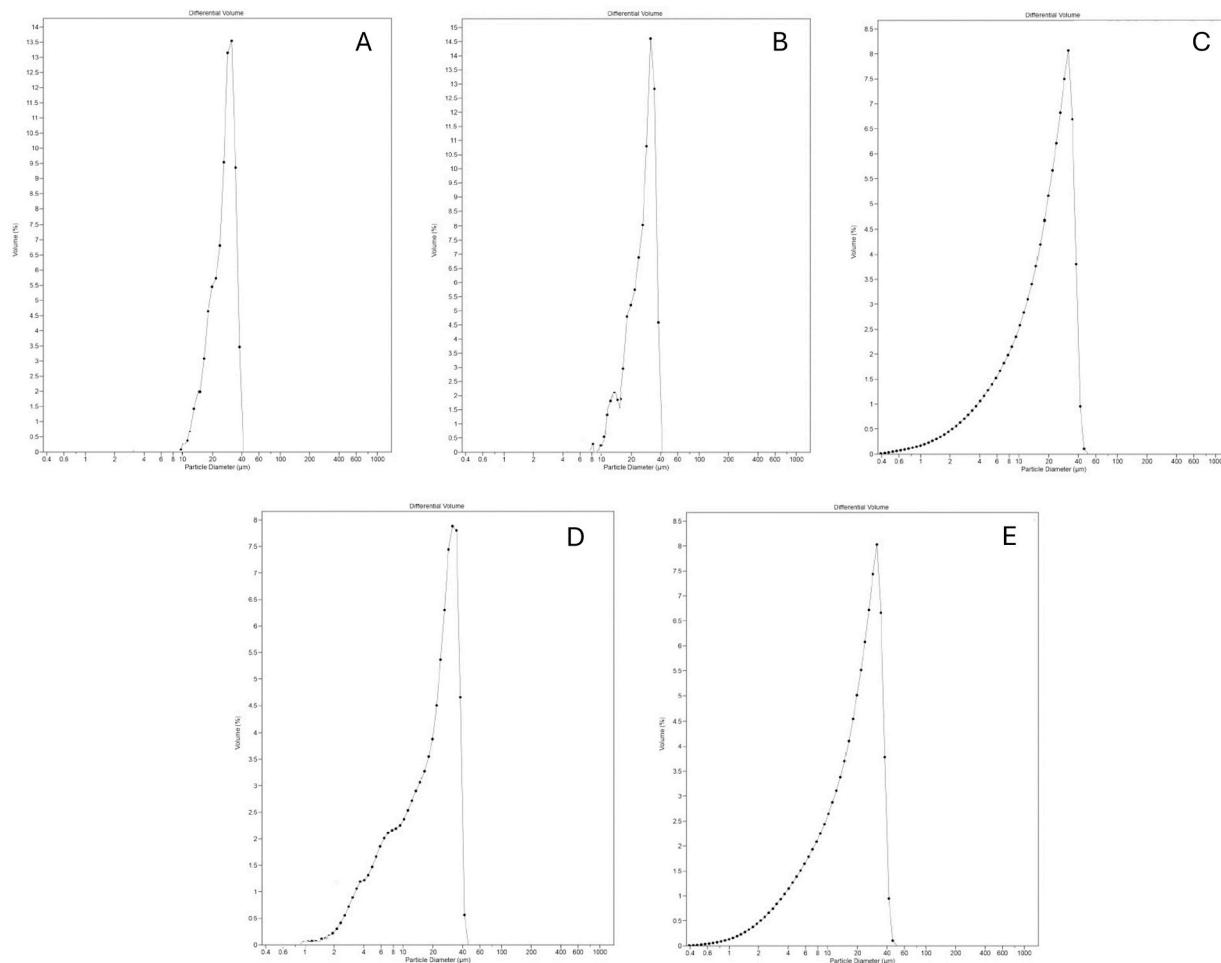


Fig. 1. LS size distribution profile of insulin dry powder (IDP) F1 (A), F2 (B), F3 (C), F4 (D), and F5 (E) with dispersion in toluene.

Table 2
Geometric diameter of IDP.

Formulation of IDP	Particle size (μm)			
	Dv10 %	Dv50 %	Dv90 %	Dv average
F1	6.45 \pm 0.21	24.64 \pm 0.74	33.98 \pm 0.91	23.03 \pm 0.67
F2	7.07 \pm 0.17	25.21 \pm 0.62	34.87 \pm 0.86	23.60 \pm 0.58
F3	4.55 \pm 0.13	19.21 \pm 0.59	33.76 \pm 0.78	19.59 \pm 0.52
F4	3.08 \pm 0.09	18.1 \pm 0.38	34.26 \pm 0.59	18.53 \pm 0.26
F5	4.56 \pm 0.15	18.96 \pm 0.61	33.73 \pm 0.75	18.77 \pm 0.51
p value	0.007	0.003	0.009	0.000

All values are presented as mean \pm standard deviation ($n = 3$). The Dv data were analyzed using One-Way ANOVA, yielding a significance value of $p < 0.05$, which indicates a significant difference in the dependent variable (Dv average) among the formulations. However, post hoc analysis with Tukey HSD revealed p-values greater than 0.05 between F1 and F2, F1 and F3, F2 and F3, as well as F4 and F5, indicating no significant differences in Dv average among these specific formulations.

the smallest dvs. These results aligned with prior research where trehalose was used as the sole positive control in cryoprotector agent investigations. The crystalline nature of the micro-particle formulations was caused by the high relative humidity of the environment and the hygroscopic nature of trehalose [31]. Differences in trehalose ratio within the formula contributed to variations in moisture content, which had a significant statistical impact on the particle size observed in the dvs among different formulas.

Some IDP formulations also exhibited non-significant differences in mean particle size ($p > 0.05$), specifically between IDP F1 and F2, as well as between IDP F4 and F5, as shown in Table 2. These outcomes are associated with the excipient composition, particularly the similar ratios of trehalose and inulin sugars among these IDP formulations. IDP F1 contains trehalose with a b/b ratio of 5:1 to inulin, similar to IDP F2 with a trehalose and inulin ratio of 2:1. On the other hand, IDP F4 and F5 also contain similar weight ratio of trehalose and inulin, specifically 1:2 and 1:5, respectively. The similarity in the trehalose and inulin ratios in these formulations results

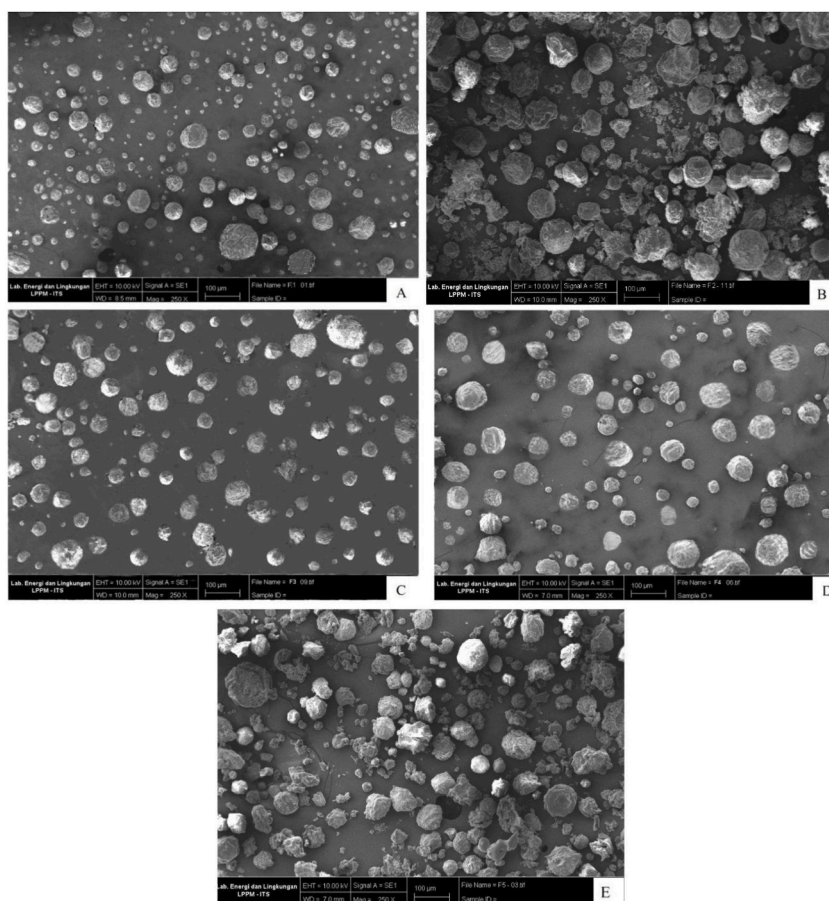


Fig. 2. The particle shape and surface properties of IDP F1 (A), F2 (B), F3 (C), F4 (D), and F5 (E) were analyzed using scanning electron microscopy (SEM) at a magnification of 250 \times .

in a resemblance in particle crystallinity and moisture content [31], which in turn contributes to the similarity in their mean particle size. The particle size is also usually influenced by process parameters in the production of dry powder, specifically in SFD, such as nozzle diameter and atomization rate, as well as differences in drying methods [32]. In this study, the process parameters were controlled variables, hence they caused no differences.

These sizes must be suitable for the criteria of delivery and administration route. In this study, IDP was designed for NTBD, requiring a specific size criterion. Particles with a diameter larger than 20 μm have been reported to be preferred for deposition in the anterior nasal cavity, while small ones with a diameter less than 5 μm could penetrate the lower respiratory tract [33]. Therefore, the main size limit considered for nasal delivery was 10 μm . Particles with a median diameter smaller than 10 μm tended to continue their journey to the lower respiratory tract and were not deposited in the nasal cavity. Additionally, those around 10 μm in diameter were best deposited in the olfactory area [34]. All seven IDP formulations met the required standards based on the particle size range of 10–60 μm for intranasal delivery.

3.1.3. Particle shape and surface

Based on Fig. 2, scanning electron microscope (SEM) data at a 250 \times magnification were used to characterize particle shape and surface. The entire five formulas of IDP were found to exhibit a spherical shape with rough surface features, aligned with prior studies employing the same drying method. SFD, involving atomization of the solution through a nozzle [29] and optimization of critical process parameters (CPPs), led to the observed spherical shape. IDP exhibited spherical-shaped particles, consistent with previous research employing the same drying method. In the intranasal microparticle formulation using both spray drying (SD) and spray-freeze drying (SFD) methods, spherical-shaped particles were obtained, aligning with the atomization process involved in SD and SFD drying methods [35].

Fig. 2(A-E) shows that all IDP formulations with varying weight ratio of trehalose and inulin exhibited a spherical morphology with a rough surface. The surface roughness was attributed to trehalose and inulin, which were combined to form a sugar glass system for insulin stabilization [18]. Additionally, the rough surface of a particle can emerge due to the influence of process parameters, including the drying method, temperature, pressure, freezing rate and atomization speed. Another study focused on formulating microparticles containing ivacaftor, colistin, and *N*-(methylpolyoxyethylene oxycarbonyl)-1,2-distearoyl-*sn*-glycero-3-phosphoethanolamine sodium salt (DSPE-PEG-OME) at a mass ratio of 1:1:1, demonstrated that the use of ultrasonic SFD also resulted in the formation of particles with rough surfaces [36]. Moreover, the material solution flow rate utilized in the IDP preparation was established at 1 mL/min, as determined in the preliminary study [18]. This adjustment required a purposeful reduction in the dispersion rate during the spraying phase. This controlled rate has the potential to affect the freezing dynamics in the SFD procedure, consequently affecting the surface properties of the resulting powdered particles. The freezing conditions inherent in the SFD also contributed to particle surface morphology. Rapid freezing conditions are likely to produce particles with smoother surfaces, whereas a more gradual freezing process is likely to yield particles with rougher surfaces [37].

3.1.4. Insulin content

Insulin content in IDP formulations ranged from 98.15 % \pm 0.79 %–101.76 % \pm 0.83 %. The highest content was detected in IDP F1, while the lowest was observed in F5 ($p < 0.05$). These results were consistent with the values obtained in the previous investigation that employed the same formulation method and combination of materials. Optimal protection was achieved through the synergistic combination of trehalose, a low-molecular-weight sugar possessing a high T_g value, and inulin, with good flexibility in coating and

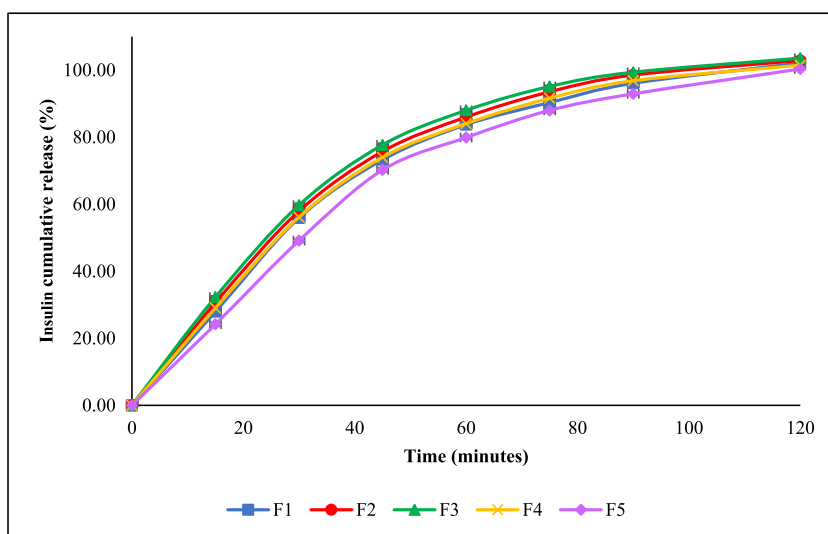


Fig. 3. The dissolution profile of insulin from dry powder formulations in phosphate buffered saline (PBS) pH 5.8. All values are presented as mean \pm standard deviation ($n = 3$).

protecting insulin [18,19]. The higher Tg value significantly contributes to the optimization of insulin stabilization. Moreover, this role ensures the absence of decrease in insulin concentration in the manufacturing process. The results were also confirmed by the highest content observed in F1, where trehalose was combined with inulin at a weight ratio of 5:1. A higher amount of trehalose would provide a better stabilizing effect due to being capable of wrapping tightly around insulin [38]. The findings align with the study conducted by Tonnis et al. (2015), in which they employed trehalose combined with dextran for formulating reconstituted insulin powder. The utilization of this combined formulation at a weight ratio of 1:1 led to increased Tg values and improved physical stability of insulin. Moreover, the insulin content in this formulation could be effectively preserved, resulting in the highest insulin content [39].

3.2. In vitro-ex vivo study of IDP

3.2.1. In vitro release study of IDP

The cumulative percentage of insulin released (%Q) was calculated to obtain the insulin release profile from the dry powder, as shown in Fig. 3. Samples were taken at 15, 30, 45, 60, 75, 90, 120, 180, and 240 min, indicating that %Q increased until 120 min, with values greater than 100 %. This result suggested the complete dissolution of all IDP formulations at 120 min, as %Q values decreased in the subsequent samples. The %Q values at 120 min ranged from 100.35 ± 0.44 to 103.58 ± 0.37 , as presented in Table 3, with the highest value being found in IDP F3 ($p < 0.05$). This result aligned with previous studies that used the same composition of materials and obtained the best formula with a trehalose and inulin ratio of 1:1, offering optimal protection, high stability, and high recovered content [18]. Moreover, the high recovered content could enhance solubility and dissolution, which correlated with high recovered content values in the stagnant layer (Cs) [40,41].

The %Q values in the first 30 and 60 min ranged between 49–60 % and 79–88 %, respectively, indicating a relatively rapid insulin release. This could be attributed to the use of water-soluble polymers, namely poloxamer, and HPMC, as excipients in the formulation of IDP. Furthermore, the IDP formulation contained entirely water-soluble ingredients. This result was consistent with previous investigations that used PVA in the formulation of mucoadhesive microspheres for intranasal insulin delivery, leading to a burst release within the first hour [42]. The pH of the formulation could affect drug solubility and its interaction with the nasal mucosa [40,41]. In this study, the pH of the dry powder formulation was adjusted to match the nasal fluid pH of 5.8, further influencing the partition coefficient, solubility, and dissolution.

The release study also aimed to analyze IDP dissolution and obtain other parameters, such as the dissolution rate constant (k), dissolution efficiency (%ED), and AUC (0–∞), as presented in Table 3. The k value was calculated following the first-order kinetic equation by plotting the remaining cumulative percentage of insulin on a logarithmic scale against time. This plot showed a strong correlation with an r^2 value greater than 0.98. The k values for all IDP formulations ranged from $(2.95 \pm 0.04) \times 10^{-2}$ to $(3.55 \pm 0.01) \times 10^{-2}$ per minute, with the highest value obtained for F3 ($p < 0.05$). Similar results were achieved for the other parameters, AUC (0–∞) and %ED, with the highest values observed for F3 at 9083.97 ± 39.75 % per minute and 73.08 ± 0.17 %, respectively. These results aligned with the highest %Q value discovered in F3, indicating that this formulation exhibited the best dissolution compared to the other four IDPs.

As previously explained, IDP F3 comprised a combination of trehalose-inulin at a weight ratio of 1:1, providing optimal physical and chemical stability. This was related to the high insulin content, which increased the Cs value and the dissolution rate. The use of excipients, particularly surfactants such as poloxamer, enhanced the dissolution process in this study, aligning with certain previously reported similar results [43]. Furthermore, the smaller particle size increased the surface area in contact with the medium, improving the dissolution rate and other dissolution parameters [40,41].

3.2.2. Ex vivo permeation study of IDP

Based on the values of recovered insulin content, the cumulative amount of insulin that permeated through the goat nasal mucosa per unit surface area of mucosa was calculated to obtain the permeation profile of IDP, as presented in Fig. 4. According to the obtained permeation profile, all IDP formulations showed a similar trend. At the 15-min sampling time, the recovered content gradually increased over time, penetrating the mucosa, indicating a non-steady-state condition. Subsequently, the diffusion rate stabilized,

Table 3

Dissolution parameters of IDP formulations.

Formula	Q _{120min} (%)	AUC _(0-∞)	Dissolution efficiency	Dissolution rate constant (k)
		(%.minutes)	(%ED)	($\times 10^{-2}$ /minutes)
F1	102.10 ± 0.52	8661.085 ± 43.04	70.69 ± 0.27	3.12 ± 0.06
F2	102.86 ± 0.30	8918.662 ± 44.42	72.26 ± 0.19	3.48 ± 0.02
F3	103.58 ± 0.37	9083.973 ± 39.75	73.08 ± 0.17	3.55 ± 0.01
F4	101.48 ± 0.37	8724.674 ± 47.51	71.65 ± 0.26	3.39 ± 0.02
F5	100.35 ± 0.44	8268.495 ± 31.00	68.67 ± 0.15	2.95 ± 0.04
p value	0.000	0.000	0.000	0.000

Q_{120min} = insulin cumulative release for 120 min. All values are presented as mean ± standard deviation ($n = 3$). All values were analyzed using One-Way ANOVA, yielding a significance value of $p < 0.05$, which indicates a significant difference in each dependent variable (Q_{120min}, AUC_(0-∞), %ED, k) among the formulations. However, post hoc analysis with Tukey HSD revealed p-values greater than 0.05 for AUC between F1 and F4, and for k between F2 and F3, as well as F2 and F4, indicating no significant differences in AUC and k among these specific formulations.

entering a steady-state condition that lasted from 30 to 240 min. At 300 and 360 min, the diffusion rate decreased, suggesting a return to a non-steady-state condition.

To analyze the permeation of IDP in goat nasal mucosa, the permeation flux value was calculated by plotting a graph that showed the relationship between the cumulative amount of insulin permeated through the nasal mucosa per cm^2 and time at a steady-state condition. Based on Fick's law, the slope of the regression equation represents the permeation rate (flux) [41]. The permeation flux and cumulative amount of insulin permeated over 6 h can be seen in Table 4.

The cumulative amount of insulin permeated over 6 h ranged from $61.73 \pm 0.54 \mu\text{g}/\text{cm}^2$ to $71.30 \pm 0.58 \mu\text{g}/\text{cm}^2$, with the highest value obtained from IDP F3 ($p < 0.05$). Similarly, the highest permeation flux value of $0.26 \mu\text{g}/\text{cm}^2/\text{minute}$ was achieved by F3 ($p < 0.05$), while the lowest flux of $0.22 \mu\text{g}/\text{cm}^2/\text{minute}$ was found in F5 ($p < 0.05$). These results were consistent with the high insulin content and dissolution parameter values discovered in the release study for F3. These also aligned with other studies that developed chitosan-based microparticles and detected a correlation between release and permeation [44].

Factors affecting the permeation of drugs from the nasal cavity to the brain include the physicochemical properties of the active pharmaceutical ingredient (API), formulation design, properties of the nasal mucosal tissue, and experimental conditions. For instance, the physicochemical properties of the API such as the lipophilicity, molecular weight, and partition coefficient can impact its permeation. These properties can influence the solubility of the active substance in nasal fluid and the ability of drugs to pass through the nasal mucosal layer [45–47]. In this study, IDP F3 with a 1:1 wt ratio of trehalose combined to inulin, showed high content and stability, enhancing the solubility of insulin in nasal fluid and consequently improving the dissolution and permeation through the nasal mucosa.

The formulation factors for NTBD include the type and proportion of excipients, production techniques, and the formulation pH. These can respectively affect the physicochemical properties and stability of the formulation, as well as drug solubility and interaction with the nasal mucosa [45–47]. Surfactants, mucoadhesives, and polymers are commonly used excipients in intranasal drug delivery formulations [48]. In this study, all formulations contained trehalose and inulin as stabilizers, poloxamer as a surfactant and permeation enhancer, and HPMC as a mucoadhesive. The application of these excipients increased insulin dissolution as evidenced by its relatively rapid release. This also boosted insulin permeation through the nasal mucosa, as demonstrated by the cumulative amount permeated within the first 30 min. However, among these excipients, the mucoadhesive polymer is the most crucial factor in the *ex vivo* permeation parameter and NTBD of insulin from IDPs. The mucoadhesive polymer can enhance the adhesion of IDP to the nasal mucosa, thereby increasing the contact time of IDP with the nasal mucosa and its permeation [47,48]. Poloxamer, which functions as both a surfactant and a permeation enhancer, enhances the release of insulin from IDP, resulting in a greater amount of insulin being released. However, if IDP does not have adequate contact time with the nasal mucosa, then the greater amount of insulin released may not necessarily result in high permeation [48]. The IDP was adjusted to the pH of the nasal fluid of 5.8, which similarly affected the partition coefficient, solubility, and dissolution, leading to enhanced permeation.

The nasal mucosa factors as controlled variables include physiological characteristics such as surface area and thickness, the presence of hydrolytic enzymes, and mucus flow. These often influence the contact time between the drug and the mucosa, as well as drug permeation ability [45–47].

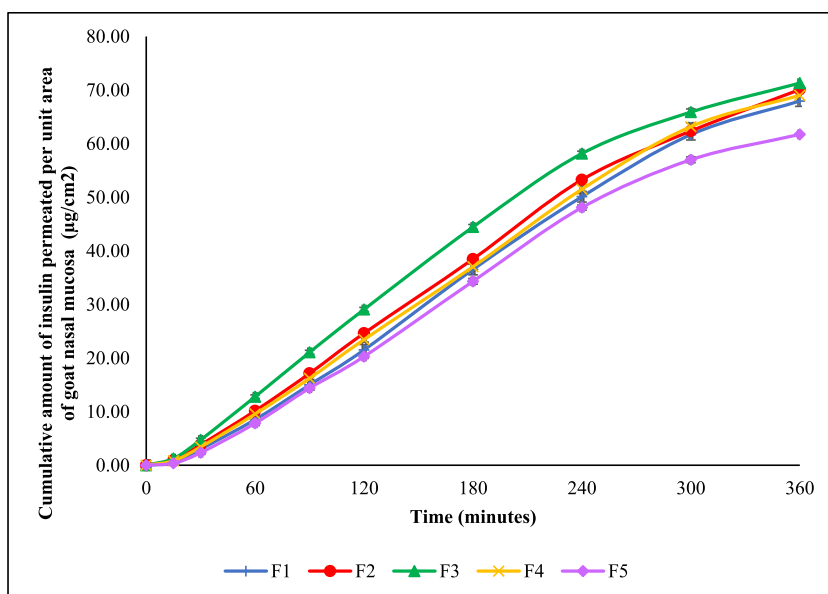


Fig. 4. Insulin permeation profile of IDPs in PBS pH 5.8. All values are presented as mean \pm standard deviation ($n = 3$).

Table 4

The cumulative amount and flux of insulin permeated from dry powder at the end of 6 h.

Formula	Insulin cumulative amount permeated at 6 h ($\mu\text{g}/\text{cm}^2$)	Flux ($\mu\text{g}/\text{cm}^2/\text{minutes}$)
F1	67.96 \pm 0.48	0.23 \pm 0.00
F2	70.10 \pm 0.47	0.24 \pm 0.00
F3	71.30 \pm 0.58	0.26 \pm 0.00
F4	69.02 \pm 0.68	0.23 \pm 0.00
F5	61.73 \pm 0.54	0.22 \pm 0.00
p value	0.000	0.000

All values are presented as mean \pm standard deviation ($n = 3$). All values were analyzed using One-Way ANOVA, yielding a significance value of $p < 0.05$, which indicates a significant difference in each dependent variable (insulin cumulative amount permeated at 6 h and flux) among the formulations. However, post hoc analysis with Tukey HSD revealed p-values greater than 0.05 for the insulin cumulative amount permeated between F1 and F4, F2 and F3, as well as F2 and F4, and for the flux between F1 and F4, indicating no significant differences in these parameters among these specific formulations.

3.2.3. Mucoadhesion study of IDP

Mucoadhesive strength was evaluated using two methods, namely *in vitro* strength testing and *ex vivo* time mucoadhesion testing, both conducted on goat nasal mucosa following the same preparation method as the permeation testing. According to Table 5, F1 and F2 needed a greater force of 230 g for the detachment of IDP plates with respective mucoadhesive times of 48.10 \pm 2.31 and 45.26 \pm 2.71 s. Conversely, F3, F4, and F5 containing smaller trehalose ratios required less force to detach from the goat nasal mucosa. This aligned with the results of *ex vivo* testing, where IDP F5 demonstrated the fastest detachment time, while F1 showed the longest ($p < 0.05$). Additionally, the detachment times for IDP formulations compressed into thin plates ranged from 20.29 \pm 0.89 to 26.14 \pm 0.39 min, as presented in Table 5.

Factors affecting the mucoadhesive properties of nasal powder formulations include their physicochemical properties and the characteristics of the mucosa [49]. In this study, differences in mucoadhesion time and strength were influenced by the IDP characteristics. The five IDPs were prepared with different ratios of trehalose and inulin, with F1 containing the highest trehalose ratio compared to the other four formulations, while F5 had the lowest. Trehalose, being more hygroscopic than inulin, conferred greater hygroscopicity and stronger mucoadhesive properties to the resulting powder [50]. Trehalose is a disaccharide consisting of two glucose molecules linked by an α , α -1,1 bond, while inulin is a fructan polysaccharide comprising several fructose molecules linked by a β , 2-1 bond. Due to its unique structure and hygroscopicity, trehalose exhibits distinct mucoadhesive strength compared to inulin [51]. The percentage of HPMC used as a mucoadhesive enhancer was kept constant in all formulations.

The characteristics of the nasal mucosa equally influence the mucoadhesive properties of IDP formulations. The structure of the nasal mucosa, comprising a mucus layer and cilia on its surface, facilitates the capture of a formulation or powder through electrostatic interactions, hydrogen bonding, and van der Waals forces. Additionally, environmental conditions within the nasal cavity, such as pH, viscosity, and flow rate, play a role in determining the mucoadhesive properties [49]. In this study, the nasal mucosa characteristics were controlled variables due to the standardized preparation of the nasal mucosa for all tests.

In summary, enhancing the mucoadhesive properties of a nasal formulation requires careful consideration of its physicochemical properties and the nasal mucosa characteristics. By considering these factors during the development of the formulations for drug delivery, optimal delivery and maximal biodistribution to the desired tissue can be achieved.

3.2.4. Ex vivo histopathology study of IDP

During the histopathological examination, goat nasal mucosa was cut into a size of approximately 0.5 cm in length, width, and thickness. The samples were treated with IDP and fixed in 10 % formalin solution for 12–24 h to evaluate the safety and potential irritation of the nasal mucosa. Subsequently, the histological images of the nasal mucosa were obtained through HE staining, as shown in Fig. 5.

The negative control treatment, which involved the administration of physiological saline solution onto the nasal mucosa,

Table 5*In vitro* mucoadhesion strengths and *ex vivo* mucoadhesion time of IDP formulations.

Formula	<i>In vitro</i> mucoadhesion		<i>Ex vivo</i> mucoadhesion
	Force (g)	Time (s)	Time (s)
F1	230	48.10 \pm 2.31	26.14 \pm 0.39
F2	230	45.26 \pm 2.71	24.21 \pm 0.39
F3	210	43.72 \pm 1.47	22.60 \pm 2.09
F4	200	48.81 \pm 2.45	20.92 \pm 2.11
F5	200	43.60 \pm 2.57	20.29 \pm 0.89
p value	–	–	0.003

All values are presented as mean \pm standard deviation ($n = 3$). All values were analyzed using One-Way ANOVA, yielding a significance value of $p < 0.05$, which indicates a significant difference in *ex vivo* mucoadhesion time among the formulations. However, post hoc analysis with Tukey HSD revealed p-values greater than 0.05 between F1 and F2, F1 and F3, F2 and F3, F2 and F4, F3 and F4, F3 and F5, as well as F4 and F5, indicating no significant differences in *ex vivo* mucoadhesion time among these specific formulations.

displayed intact and normal epithelial structures with a lesion score of 0, indicating no damage or irritation, as seen in Fig. 5(A). In contrast, the positive control treatment with isopropyl alcohol initiated epithelial damage in the upper layer (Fig. 5(B)) with a lesion score of 2. Treatments with all IDP formulations resulted in observations similar to the negative control, with epithelial lesion scores of

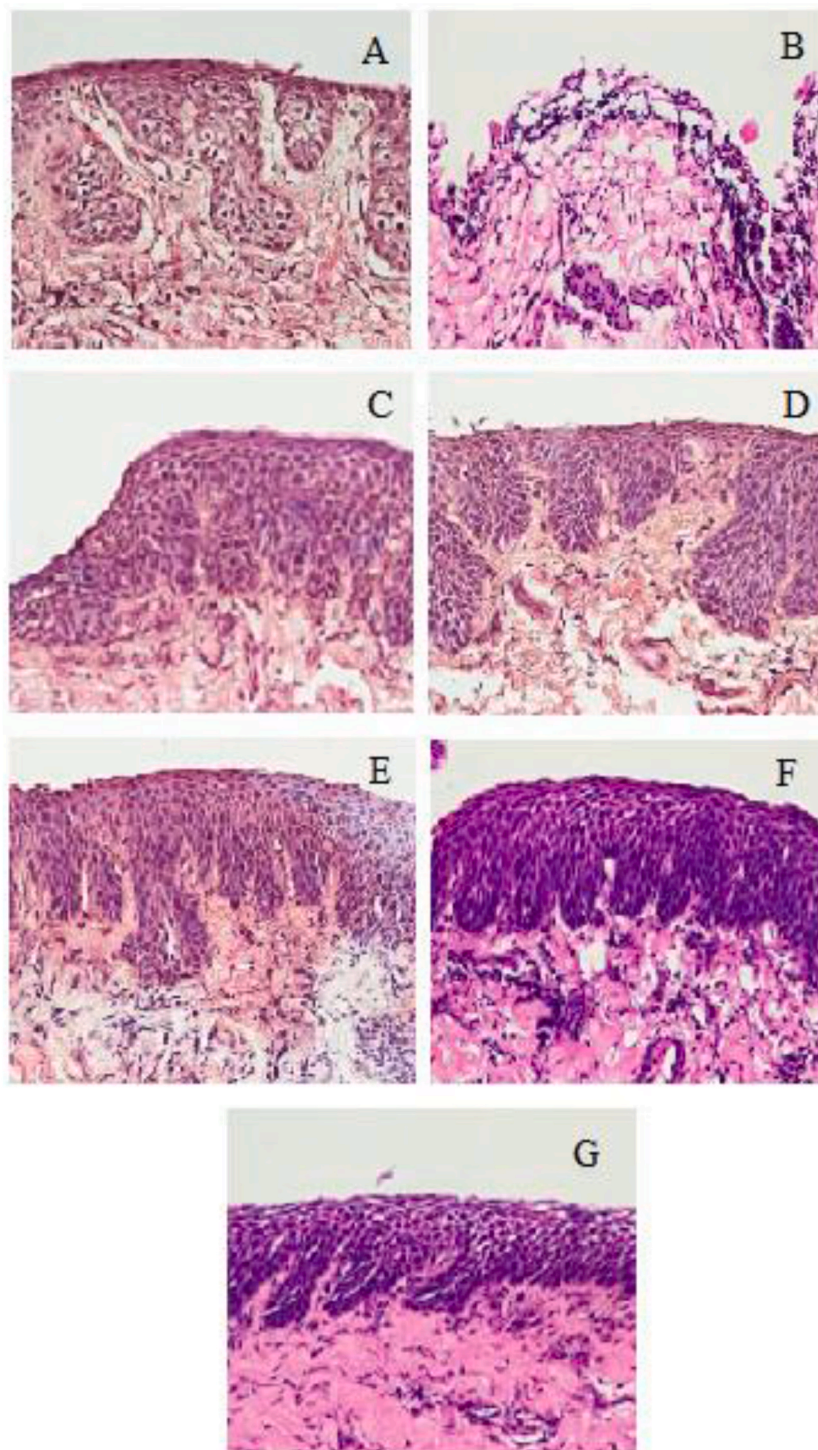


Fig. 5. The hematoxylin-eosin (HE) staining of nasal mucosa in the histopathological examination after treatment, including the negative control (A), positive control (B), and IDP formulations F1 (C), F2 (D), F3 (E), F4 (F), and F5 (G), demonstrated the absence of mucosal damage or irritation following IDP administration.

0, indicating no nasal damage or irritation, as seen in Fig. 5(C-G).

Particle size is an important factor affecting the safety of dry powder formulations. Extremely large particles often cause physical irritation to the mucosal surface, while very small ones can lead to systemic absorption and potential toxicity [33]. In this study, all IDP formulations had diameters ranging from 18.46 to 23.60 μm , suitable for NTBD through the olfactory pathway. Based on this particle size, the IDPs are not supposed to irritate the nasal mucosa.

The choice of excipients in dry powder formulations can also influence safety and tolerability. Excipients such as surfactants, preservatives, and stabilizers, are commonly employed to improve the physical and chemical stability of the formulation. Previous studies using trehalose in ovalbumin nasal powder formulations obtained particles with a diameter ranging from 16 to 20 μm . A histopathological examination performed on the nasal lymphatic tissue of monkeys showed normal epithelial cells in the vestibular, olfactory, and respiratory regions based on HE staining. Additionally, the distribution of the powder formulation was better in the anterior nasal region compared to the liquid formulation, indicating that trehalose in the ovalbumin powder formulation did not induce irritation in the nasal lymphatic tissue [52]. In this study, apart from trehalose, excipients such as inulin, HPMC, and poloxamer were added to IDP. Another exploration of an intranasal nano-vaccine delivery system based on inulin acetate demonstrated its safety and potential for mucosal intranasal vaccine delivery [53]. HPMC and poloxamer are commonly used in the development of lipid-based nanoparticles for NTBD [54]. In-depth histopathological and biomarker testing in rats confirmed the safety of this formulation, as evidenced by the absence of nasal mucosal damage, such as cell necrosis or loss of cilia [55]. Overall, the entire excipients applied in the examined IDP formulations demonstrated safety and tolerability, leading to being suitable for intranasal administration.

The pH of dry powder formulations is another crucial factor affecting their safety and tolerability. The nasal mucosa is slightly acidic, hence its surface can be irritated or damaged by formulations with an extremely high or low pH [56]. In this study, all IDP formulations were adjusted to pH 5.8, consistent with the physiological pH of nasal fluids. In another study, the administration of a combination of plant gum and the infectious bursal disease virus (IBDV) vaccine via ocular route showed no signs of irritation. In another group that received the vaccine or plant gum alone, lesions were observed. This was influenced by the pH of the formulation and its compatibility with ocular physiological conditions [57].

Factors such as dose, frequency of administration, and duration of treatment, can influence the risk of local irritation and systemic toxicity. In this study, the dosing and administration frequency were controlled, and no significant irritation or damage to the nasal mucosa was observed.

3.2.5. *In vivo* biodistribution study of IDP

The *in vivo* biodistribution study provided valuable insights into the distribution and recovered content of insulin in the olfactory region and brain following intranasal administration of the IDP formulations. This aimed to evaluate the transport and delivery of insulin to the target sites.

The deposited insulin concentration in the tissues or plasma was calculated as an amount of insulin (μIU) in the weight of the tissues, as shown in Fig. 6. Fig. 6(A) shows the amount of insulin deposited in the olfactory bulb, while Fig. 6(B) shows the amount of insulin deposited in the whole brain at 15, 60, 90, and 120 min after administration. Insulin from IDP F1–F5 was not detected in the plasma until 120 min after administration (data not presented), indicating that the IDP intranasal delivery did not lead to the systemic circulation of insulin.

Insulin administered through the intranasal route often bypasses the blood-brain barrier and reaches the brain directly, thereby increasing treatment effectiveness. This approach is particularly advantageous for AD therapy, as systemic circulation of the hormone is not required, circumventing the limitations associated with insulin that does not reach systemic circulation [58]. Several factors contribute to the low systemic circulation of intranasally delivered insulin, including biological factors and drug formulation [59].

Biological factors contributing to the low systemic circulation of insulin include the presence of hydrolytic enzymes in the nasal

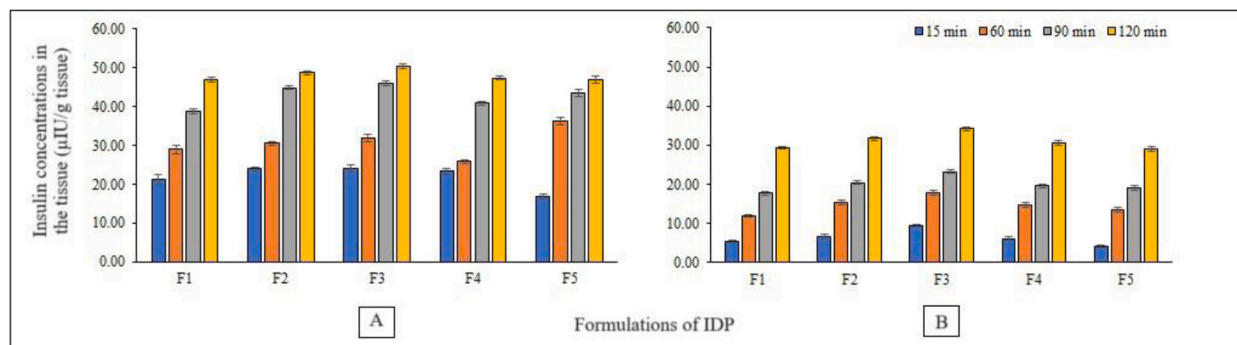


Fig. 6. The deposited insulin concentration ($\mu\text{IU/g}$ tissue) in the olfactory bulb (A) and whole brain (B) after intranasal administration. The blank samples, which consisted of PBS pH 5.8, were observed as the normal control for each intranasal administration time point, resulting in undetected insulin concentration in plasma, olfactory bulb, and whole brain (data not shown). All IDP administrations also yielded undetected insulin levels in the plasma (data not shown). All values are presented as mean \pm standard deviation ($n = 3$).

mucosa. The high enzymatic activity in the nasal mucosa rapidly degrades insulin before entering the systemic circulation. Additionally, the highly vascularized nasal mucosa allows insulin absorbed to be directly transported to the brain through the olfactory nerves, limiting systemic distribution [58].

Drug formulation factors influencing the low systemic circulation of insulin include the use of mucoadhesive agents, such as carbopol or polyacrylate, which can increase the retention time of insulin in the nasal cavity and enhance its absorption [58,59]. These mucoadhesive agents tend to promote insulin absorption by the nasal mucosa, reducing systemic distribution. In this study, HPMC E5 served as the mucoadhesive agent, contributing to increased insulin retention in the nasal cavity and decreased systemic distribution [60,61]. This aligned with a previous study that used L-penetratin and D-penetratin in liquid insulin formulations for intranasal delivery, both of which demonstrated significant effects on insulin biodistribution in the olfactory bulb and brain compared to formulations without these agents. Furthermore, the use of D-penetratin demonstrated a minimal risk of side effects on systemic circulation [28].

In the olfactory bulb, deposited insulin concentration ranged from $46.94 \pm 0.934 \mu\text{IU/g}$ tissue to $50.35 \pm 0.75 \mu\text{IU/g}$ tissue after 120 min, while insulin lower concentration of $29.05 \pm 0.70 \mu\text{IU/g}$ tissue to $34.21 \pm 0.55 \mu\text{IU/g}$ tissue was observed in the whole brain, as shown in Fig. 6. These results indicated that insulin can be adequately distributed within the olfactory bulb and brain. Among the dry powder formulations, F3 demonstrated the highest deposited insulin concentration reaching $50.35 \pm 0.75 \mu\text{IU/g}$ tissue in the olfactory bulb and $34.21 \pm 0.55 \mu\text{IU/g}$ tissue in the brain after 120 min of administration ($p < 0.05$). This corresponded to the high amount of insulin found in F3.

Nasal delivery of insulin permits targeted distribution to the olfactory region and brain while avoiding systemic circulation. This aligns with the objective of delivering insulin directly to the brain for AD therapy. The distribution of insulin to the olfactory bulb and brain is influenced by several factors, including the physicochemical properties of insulin, characteristics of the nasal mucosa, and the form and formulation of the drug [59].

In this study, insulin was formulated as a micro-sized dry powder, further influencing its distribution to the brain. All IDP formulations (F1–F5) demonstrated significant biodistribution to the olfactory region and brain compared to systemic circulation. The physical and chemical characteristics of insulin play a significant role in its distribution to the olfactory region and brain. Smaller insulin molecules exhibit a greater ability to cross the blood-brain barrier and reach the brain. Therefore, chemically modified insulin with reduced molecular size can enhance distribution to the brain [59].

The characteristics of the nasal mucosa, such as permeability and vascularity, influence insulin distribution to the olfactory region and brain. A more permeable and vascular nasal mucosa enhances insulin absorption and distribution to the brain [58]. In this study, the nasal mucosa was controlled using the same preparation method for all treatments, ensuring it was a controlled variable.

The form and formulation of the drug also impact insulin distribution to the olfactory region and brain. Formulations that adhere to the nasal mucosa or contain absorption enhancers can increase insulin distribution to the brain while reducing systemic distribution [58,59]. The present study demonstrated similar results, where all dry powder formulations (F1–F5) exhibited undetectable systemic biodistribution, while significant biodistribution was observed in the olfactory region and brain. This result aligned with previous studies that formulated insulin with L-penetratin and D-penetratin. Low biodistribution of insulin has been reported in liquid formulations without the two components, while the addition of both components significantly enhanced insulin biodistribution to the olfactory region and brain. The use of these two excipients minimized the risk of side effects in systemic circulation [28].

The factors influencing insulin biodistribution to the brain through nasal delivery are not fully understood, including the specific routes and mechanisms involved. Various routes have been proposed for the targeted transportation of compounds from the nasal passage specifically to the brain [62,63]. The major pathway is believed to encompass axonal transportation throughout the olfactory or trigeminal nerves across the olfactory and respiratory mucosa [64–67]. These transport pathways associated with the olfactory and trigeminal nerves extend to the olfactory bulb and brainstem, potentially requiring endocytosis for the transport of bioactive macromolecules. An alternative pathway includes permeation processes through the epithelial cells supporting the olfactory and respiratory mucosa, comprising extracellular diffusion and transcytosis. Molecules that penetrate the lamina propria layer subsequently diffuse into the cerebrospinal fluid (CSF) through perineural passages or flow collectively into the perivascular region [62,63]. Molecules conveyed to the olfactory bulb, brainstem, or CSF are anticipated to ultimately access the brain parenchyma.

According to the transport mechanisms suggested in existing literature [62–67], the initial phase in the complete transport pathway from the nasal passages to the brain involves drug absorption by the nasal epithelium, including uptake by neuronal and supporting cells. As previously explained, achieving adequate insulin concentrations specifically in the brain may not be accomplished solely through intranasal administration without additional delivery approaches. To assure the therapeutic effectiveness of intranasally administered insulin in the brain, the key challenge lies in promoting effective transportation from the nasal passages specifically to the brain. Furthermore, previous studies by Kamei & Takeda-Morishita demonstrated the use of L-penetratin and D-penetratin to be capable of augmenting insulin levels in the olfactory region and brain. This observation suggests that penetration-enhancing compounds can increase insulin accumulation in the brain [28].

Further biodistribution testing of insulin in specific brain regions can be conducted. The brain consists of various specific regions, such as medulla oblongata, pons, cerebellum, thalamus, hypothalamus, amygdala, hippocampus, and cortex, each with distinct roles and functions. The cortex is subdivided into several parts, including the frontal lobe, parietal lobe, temporal lobe, and occipital lobe. Brain regions associated with AD include the hippocampus and cortex [68]. Biodistribution testing of insulin in specific brain regions can provide further analysis of its relevance to the effectiveness of AD therapy.

4. Conclusion

The comprehensive evaluations of the IDP formulations through *in vitro*, *ex vivo*, and *in vivo* studies suggest that the produced IDPs have their potential for non-invasive NTBD. Among the tested IDP formulations, F3 with a weight ratio of trehalose to inulin of 1:1, demonstrated the most promising results of brain biodistribution. Therefore, F3 was recommended for further exploration and development in NTBD. Subsequent studies should focus on assessing various excipients, including penetrating agents, to improve their *in vivo* performance and safety. This formulation can be further extended to investigate dosing and multiple administrations of IDP intranasally, which are essential to ensure the effectiveness and safety of repeated IDP administration. In addition, similar assessments on commercial liquid insulin products need to be conducted in future studies to compare their *in vitro*, *ex vivo*, and *in vivo* biodistribution aspects with those of IDP. Further comparison can then be analyzed to optimize stable IDP formulations suitable for NTBD. The results will contribute valuable insights to the development of novel therapeutic strategies for neurodegenerative diseases, such as AD, utilizing the advantages of intranasal drug delivery.

Ethics statement

The biodistribution study of IDP in rats adhered to ethical guidelines as approved by the Institutional Ethical Committee of the University of Surabaya (Approval Number 227/KE/XII/2021).

Data availability statement

The data supporting the results of this study are included in article and available upon request.

CRedit authorship contribution statement

Cynthia Marisca Muntu: Writing – review & editing, Writing – original draft, Visualization, Software, Resources, Project administration, Methodology, Funding acquisition, Formal analysis, Data curation, Conceptualization. **Christina Avanti:** Writing – review & editing, Methodology, Investigation. **Hayun:** Writing – review & editing, Methodology, Investigation. **Silvia Surini:** Writing – review & editing, Validation, Supervision, Methodology, Investigation, Funding acquisition, Data curation.

Declaration of competing interest

The authors declare that they have no known competing financial interests or personal relationships that could have appeared to influence the work reported in this paper.

Acknowledgments

We would like to express our gratitude to the University of Indonesia and the University of Surabaya for their invaluable support in completing this research project.

References

- [1] Z. Wang, G. Xiong, W.C. Tsang, A.G. Schätzlein, I.F. Uchegbu, Nose-to-Brain delivery, *J. Pharmacol. Exp. Therapeut.* 370 (3) (2019) 593–601, <https://doi.org/10.1124/jpet.119.258152>.
- [2] W. Alabsi, B.B. Eedara, D. Encinas-Basurto, R. Polt, H.M. Mansour, Nose-to-Brain delivery of therapeutic peptides as nasal aerosols, *Pharmaceutics* 14 (9) (2022) 1870, <https://doi.org/10.3390/pharmaceutics14091870>.
- [3] Y. Li, S. Kanzaki, S. Shibata, M. Nakamura, M. Ozaki, H. Okano, K. Ogawa, Comparison of drug availability in the inner ear after oral, transtympanic, and combined administration, *Front. Neurol.* 12 (2021), <https://doi.org/10.3389/fneur.2021.641593>.
- [4] Z.H. Ali, M. Alkotaji, Nose to brain delivery of drugs for CNS diseases, *Iraqi. J. Pharm.* 18 (1) (2021) 93–107, <https://doi.org/10.33899/iph.2021.168804>.
- [5] Alzheimer's Association, Alzheimer's disease facts and figures, *Alzheimers Dement* 15 (2019) 321–387.
- [6] M. Kvello-Alme, G. Bråthen, L.R. White, S.B. Sando, Time to diagnosis in young onset Alzheimer's disease: a population-based study from Central Norway, *J. Alzheimers Dis.* 82 (3) (2021) 965–974.
- [7] A. Atri, Current and future treatments in Alzheimer's disease, *Semin. Neurol.* 39 (2) (2019) 227–240.
- [8] T.M. Hughes, S. Craft, The role of insulin in the vascular contributions to age-related dementia, *Biochim. Biophys. Acta* 1862 (2016) 983–991.
- [9] S. Kullmann, M. Heni, M. Hallschmid, A. Fritsche, H. Preissl, H.U. Häring, Brain insulin resistance at the crossroads of metabolic and cognitive disorders in humans, *Physiol. Rev.* 96 (4) (2016) 1169–1209.
- [10] A.A. Akintola, D. van Heemst, Insulin, aging, and the brain: mechanisms and implications, *Front. Endocrinol.* 6 (2015) 13.
- [11] M. Muñoz-Jiménez, A. Zaarkti, J.A. García-Arnés, N. García-Casares, Antidiabetic drugs in alzheimer's disease and mild cognitive impairment: a systematic review, *Dement. Geriatr. Cogn. Disord* 49 (5) (2021) 423–434.
- [12] S. Craft, L.D. Baker, T.J. Montine, et al., Intranasal insulin therapy for alzheimer disease and amnesic mild cognitive impairment: a pilot clinical trial, *Arch. Neurol.* 69 (1) (2012) 29–38, <https://doi.org/10.1001/archneurol.2011.233>.
- [13] M.A. Reger, G.S. Watson, P.S. Green, et al., Intranasal insulin administration dose-dependently modulates verbal memory and plasma amyloid-beta in memory-impaired older adults, *J. Alzheimers Dis.* 13 (2008) 323–331, <https://doi.org/10.3233/jad-2008-13309>.
- [14] P. Picone, M.A. Sabatino, L.A. Ditta, A. Amato, P.L.S. Biagio, F. Mulè, D. Giacomazza, C. Dispenza, M.D. Carlo, Nose-to-brain delivery of insulin enhanced by a nanogel carrier, *J. Contr. Release* 270 (2018) 23–36.
- [15] L. Heinemann, K. Braune, A. Carter, A. Zayani, L.A. Kramer, Insulin storage: a critical reappraisal, *J. Diabetes Sci. Technol.* 15 (1) (2021) 147–159.
- [16] S. Bahendeka, R. Kaushik, A.B. Swai, F. Otieno, S. Bajaj, S. Kalra, C.M. Bavuma, C. Karigire, EADSG Guidelines : insulin storage and optimisation of injection technique in diabetes management, *Diabetes Therapy, Springer Healthcare* 10 (2) (2019) 341–366, <https://doi.org/10.1007/s13300-019-0574-x>.

- [17] FDA. <https://www.fda.gov/>, 2019. (Accessed 6 June 2021).
- [18] C.M. Muntu, S. Surini, C. Avanti, Hayun, Preliminary study of insulin dry powder formulation: critical process parameters on spray-freeze-drying and critical material attributes of trehalose and inulin as stabilizers, *Int. J. Appl. Pharm.* 13 (4) (2021) 83–88, <https://doi.org/10.22159/ijap.2021.v13s4.43823>.
- [19] C.M. Muntu, C. Avanti, H. Hayun, S. Surini, Stability study of spray freeze-dried insulin dry powder formulations used for nose-to-brain delivery, *J. Appl. Pharmaceut. Sci.* 13 (10) (2023) 225–237, <https://doi.org/10.7324/JAPS.2023.148983>.
- [20] S. Surini, H. Akiyama, M. Morishita, T. Nagai, K. Takayama, Release phenomena of insulin from an implantable device composed of a polyion complex of chitosan and sodium hyaluronate, *J. Contr. Release* 90 (2003) 291–301, [https://doi.org/10.1016/s0168-3659\(03\)00196-2](https://doi.org/10.1016/s0168-3659(03)00196-2).
- [21] V. Trotta, B. Pavan, L. Ferraro, S. Beggiato, D. Traini, L.G.D. Reis, S. Scalia, A. Dalpiatz, Brain targeting of resveratrol by nasal administration of chitosan-coated lipid microparticles, *Eur. J. Pharm. Biopharm.* 127 (2018) 250–259, <https://doi.org/10.1016/j.ejpb.2018.02.010>.
- [22] U. Seju, A. Kumar, K.K. Sawant, Development and evaluation of olanzapine-loaded PLGA nanoparticles for nose-to-brain delivery: *In vitro* and *in vivo* studies, *Acta Biomater.* 7 (12) (2011) 4169–4176, <https://doi.org/10.1016/j.actbio.2011.07.025>.
- [23] S.B. Yarragudi, *Formulation Strategies to Enhance Nose-To-Brain Delivery of Drugs*, 2018 (June).
- [24] S. Surini, F. Gotalia, K.S.S. Putri, Formulation of mucoadhesive buccal films using pregelatinized cassava starch phthalate as a film-forming polymer, *Special Issue, Int. J. Appl. Pharm.* 10 (1) (2018) 225–229, <https://doi.org/10.22159/ijap.2018.v10s1.50>.
- [25] Z. Yang, Y. Zhang, Z. Wang, K. Wu, J. Lou, X. Qi, Enhanced brain distribution and pharmacodynamics of rivastigmine by liposomes following intranasal administration, *Int. J. Pharm.* 452 (1–2) (2013) 344–354, <https://doi.org/10.1016/j.ijpharm.2013.05.009>.
- [26] B. Shah, D. Khunt, M. Misra, H. Padh, Application of Box-Behnken design for optimization and development of quetiapine fumarate loaded chitosan nanoparticles for brain delivery via intranasal route, *Int. J. Biol. Macromol.* 89 (2016) 206–218, <https://doi.org/10.1016/j.ijbiomac.2016.04.076>.
- [27] L.C.S. Kovalhuk, E.Q. Telles, M.N. Lima, N.A.R. Filho, Nasal lavage cytology and mucosal histopathological alterations in patients with rhinitis, *Braz. J. Otorhinolaryngol.* 86 (4) (2020) 434–442, <https://doi.org/10.1016/j.bjorl.2019.01.005>.
- [28] N. Kamei, M. Takeda-morishita, Brain delivery of insulin boosted by intranasal coadministration with cell-penetrating peptides, *J. Contr. Release* 197 (2015) 105–110, <https://doi.org/10.1016/j.jconrel.2014.11.004>.
- [29] H. Isleroglu, I. Turker, Particle morphology of spray-freeze dried microencapsulation agents, *Int. J. Sci. Technol. Res.* 5 (2) (2019) 199–206, <https://doi.org/10.7176/JSTR/5-2-24>.
- [30] M.A. Mumuni, F. C Kenchekwu, O.C. Ernest, A.M. Oluseun, B. Abdulmumin, D.C. Youngson, O.C. Kenneth, A.A. Anthony, Surface-modified mucoadhesive microparticles as a controlled release system for oral delivery of insulin, *Heliyon* 5 (9) (2019) e02366, <https://doi.org/10.1016/j.heliyon.2019.e02366>, 1–9.
- [31] W.L.J. Hinrichs, M. Prinsen, H. Frijlink, Inulin glasses for the stabilization of therapeutic proteins, *Int. J. Pharm.* 215 (1–2) (2001) 163–174.
- [32] A.D. Brunaugh, T. Wu, S.R. Kanapuram, H.D.C. Smyth, Effect of particle formation process on characteristics and aerosol performance of respirable protein powders, *Mol. Pharm.* 16 (10) (2019) 4165–4180, <https://doi.org/10.1021/acs.molpharmaceut.9b00496>.
- [33] M. Pozzoli, P. Rogueda, B. Zhu, T. Smith, P.M. Young, D. Traini, F. Sonvico, Dry powder nasal drug delivery: challenges, opportunities and a study of the commercial Teijin Pulvizer Rhinocort device and formulation, *Drug Dev. Ind. Pharm.* 42 (10) (2016) 1660–1668, <https://doi.org/10.3109/03639045.2016.1160110>.
- [34] C. Rigaut, L. Deruyver, J. Goole, B. Haut, P. Lambert, Instillation of a dry powder in nasal casts: parameters influencing the olfactory deposition with uni- and Bi-directional devices, *Front. Med. Technol. Sec. Nano-Based Drug Delivery.* 4 (2022), <https://doi.org/10.3389/fmedt.2022.924501>.
- [35] A. Di, S. Zhang, X. Liu, Z. Tong, S. Sun, Z. Tang, X.D. Chen, W.D. Wu, Microfluidic spray dried and spray freeze dried uniform microparticles potentially for intranasal drug delivery and controlled release, *Powder Technol.* 379 (2021) 144–153, <https://doi.org/10.1016/j.powtec.2020.10.061>.
- [36] S. Yu, X. Pu, M.U. Ahmed, H. Yu, T.T. Mutukuri, J. Li, Q.T. Zhou, Spray-freeze-dried inhalable composite microparticles containing nanoparticles of combinational drugs for potential treatment of lung infections caused by *Pseudomonas aeruginosa*, *Int. J. Pharm.* 610 (2021) 121160, <https://doi.org/10.1016/j.ijpharm.2021.121160>.
- [37] Z. Li, Morphology of particle produced by spray-freeze drying, *Hua Gong Jin Zhan* 32 (2013) 270–275.
- [38] M.A. Mensink, H.W. Frijlink, K.V. Maarschalk, W.L.J. Hinrichs, How sugars protect proteins in the solid state and during drying (review): mechanisms of stabilization in relation to stress conditions, *Eur. J. Pharm. Biopharm.* 114 (2017) 288–295, <https://doi.org/10.1016/j.ejpb.2017.01.024>.
- [39] W.F. Tonnis, M.A. Mensink, A. de Jager, K.V. Maarschalk, H.W. Frijlink, W.L.J. Hinrichs, Size and molecular flexibility of sugars determine the storage stability of freeze-dried proteins, *Mol. Pharm.* 12 (3) (2015) 684–694.
- [40] L. Shargel, A.B.C. Yu, in: *Applied Biopharmaceutics and Pharmacokinetics Seventh Edition* (7), Mc Graw-Hill Education, New York, 2016.
- [41] P.J. Sinko, *Martin's Physical Pharmacy and Pharmaceutical Sciences: Physical Chemical and Biopharmaceutical Principles in the Pharmaceutical Sciences*, seventh ed., Wolters Kluwer, 2017.
- [42] S.N. Zadeh, S. Rajabnezhad, M. Zandkarimi, et al., Mucoadhesive microspheres of chitosan and polyvinyl alcohol as a carrier for intranasal delivery of insulin: *in vitro* and *in vivo* studies, *MOJ. Bioequiv. Availab.* 3 (2) (2017) 39–45, <https://doi.org/10.15406/mojbb.2017.03.00030>.
- [43] D. Monti, S. Burgalassi, M.S. Rossato, B. Albertini, N. Passerini, L. Rodriguez, P. Chetoni, Poloxamer 407 microspheres for orotranasal drug delivery. Part II: *In vitro/in vivo* evaluation, *Int. J. Pharm.* 400 (1–2) (2010) 32–36, <https://doi.org/10.1016/j.ijpharm.2010.08.018>.
- [44] C.M. Spagnol, A.M. Zaera, V.L.B. Isaac, M.A. Corrêa, H.R.N. Salgado, Release and permeation profiles of spray-dried chitosan microparticles containing caffeic acid, *Saudi Pharmaceut. J.* 26 (3) (2018) 410–415, <https://doi.org/10.1016/j.jsps.2017.12.021>.
- [45] P.S. Appasaheb, S.D. Manohar, S.R. Bhanudas, A review on intranasal drug delivery system, *J. Adv. Pharm. Educ. Res.* 3 (4) (2013) 333–346.
- [46] D. Patel, H. Thakkar, Formulation considerations for improving intranasal delivery of CNS acting therapeutics, *Ther. Deliv.* 13 (7) (2022) 371–381, <https://doi.org/10.4155/tde-2022-0018>.
- [47] M. Parvathi, Intranasal drug delivery to brain: an overview, *Int. J. Res. Pharm. Chem.* 2 (3) (2012) 889–895.
- [48] M.L. Formica, D.A. Real, M.L. Picchio, E. Catlin, R.F. Donnelly, A.J. Paredes, On a highway to the brain: a review on nose-to-brain drug delivery using nanoparticles, *Appl. Mater. Today* 29 (2022) 2352–9407, <https://doi.org/10.1016/j.apmt.2022.101631>, 101631.
- [49] S. Alawdi, A.B. Solanki, Mucoadhesive drug delivery systems: a review of recent developments, *Journal of Scientific Research in Medical and Biological Sciences (JSRMSB)* 2 (2021) 1, <https://doi.org/10.47631/jsrmsb.v2i1.213>.
- [50] K.Y. Wong, Y.Y. Thoo, C.P. Tan, L.F. Siow, Moisture absorption behavior and thermal properties of sucrose replacer mixture containing inulin or polydextrose, *Appl. Food Res.* 2 (1) (2022) 100089, <https://doi.org/10.1016/j.afres.2022.100089>.
- [51] M.A. Mensink, H.W. Frijlink, K.V.D.V. Maarschalk, W.L.J. Hinrichs, Inulin, a flexible oligosaccharide. II: review of its pharmaceutical applications, *Carbohydr. Polym.* 134 (2015) 418–428, <https://doi.org/10.1016/j.carbpol.2015.08.022>.
- [52] Y. Torikai, Y. Sasaki, K. Sasaki, A. Kyuno, S. Haruta, A. Tanimoto, Evaluation of systemic and mucosal immune responses induced by a nasal powder delivery system in conjunction with an OVA antigen in cynomolgus monkeys, *J. Pharmacol. Sci. (Tokyo, Jpn.)* 110 (5) (2021) 2038–2046, <https://doi.org/10.1016/j.xphs.2020.11.023>.
- [53] M.A. Bakkari, C.K. Valiveti, R.S. Kaushik, H. Tummala, Toll-like receptor-4 (TLR4) agonist-based intranasal nanovaccine delivery system for inducing systemic and mucosal immunity, *Mol. Pharm.* 18 (6) (2021) 2233–2241, <https://doi.org/10.1021/acs.molpharmaceut.0c01256>.
- [54] T.T. Nguyen, H.J. Maeng, Pharmacokinetics and pharmacodynamics of intranasal solid lipid nanoparticles and nanostructured lipid carriers for nose-to-brain delivery, *Pharmaceutics* 14 (3) (2022) 572, <https://doi.org/10.3390/pharmaceutics14030572>.
- [55] N.A.H.A. Youssef, A.A. Kassem, R.M. Farid, F.A. Ismail, M.A.E. El-Massik, N.A. Boraie, A novel nasal almotriptan loaded solid lipid nanoparticles in mucoadhesive in situ gel formulation for brain targeting: preparation, characterization and *in vivo* evaluation, *Int. J. Pharm.* 548 (2018) 609–624, <https://doi.org/10.1016/j.ijpharm.2018.07.014>.
- [56] P.C. Pires, M. Rodrigues, G. Alves, A.O. Santos, Strategies to improve drug strength in nasal preparations for brain delivery of low aqueous solubility drugs, *Pharmaceutics* 14 (3) (2022) 588, <https://doi.org/10.3390/pharmaceutics14030588>.
- [57] G.A. Adeniran, T.A. Jarikre, O.O. Ola, O. Adigun, M.A. Odeniyi, B.O. Emikpe, Clinical and pathological responses of broilers to ocular vaccination using plant gum delivery and challenge with infectious bursal disease virus, *Comp. Clin. Pathol.* 29 (2020) 721–727, <https://doi.org/10.1007/s00580-020-03122-y>.

- [58] J.T. Trevino, R.C. Quispe, F. Khan, V. Novak, Non-invasive strategies for nose-to-brain drug delivery, *J. Clin. Trials* 10 (7) (2020) 439. <https://doi.org/10.1016/j.jcltr.2020.07.001>.
- [59] M.L. Formica, D.A. Real, M.L. Picchio, E. Catlin, R.F. Donnelly, A.J. Paredes, On a highway to the brain: a review on nose-to-brain drug delivery using nanoparticles, *Appl. Mater. Today* 29 (2022) 101631. <https://doi.org/10.1016/j.apmt.2022.101631>.
- [60] U. Anand, T.U.R. Feridooni, Novel mucoadhesive polymers for nasal drug delivery, in: *Recent Advances in Novel Drug Carrier Systems*, InTech, 2012, <https://doi.org/10.5772/52560>.
- [61] M. Trenkel, R. Scherließ, Nasal powder formulations: in-vitro characterisation of the impact of powders on nasal residence time and sensory effects, *Pharmaceutics* 13 (2021) 385. <https://doi.org/10.3390/pharmaceutics13030385>.
- [62] S.V. Dhuria, L.R. Hanson, W.H. Frey II, Intranasal delivery to the central nervous system: mechanisms and experimental considerations, *J. Pharmacol. Sci. (Tokyo, Jpn.)* 99 (2010) 1654–1673. <https://doi.org/10.1002/jps.21924>.
- [63] J.J. Lochhead, R.G. Thorne, Intranasal delivery of biologics to the central nervous system, *Adv. Drug Deliv. Rev.* 64 (2012) 614–628. <https://doi.org/10.1016/j.addr.2011.11.002>.
- [64] R.G. Thorne, G.J. Pronk, V. Padmanabhan, W.H. Frey II, Delivery of insulin-like growth factor-1 to the rat brain and spinal cord along olfactory and trigeminal pathways following intranasal administration, *Neuroscience (San Diego, CA, U. S.)* 127 (2004) 481–496. <https://doi.org/10.1016/j.neuroscience.2004.05.029>.
- [65] R.G. Thorne, L.R. Hanson, T.M. Ross, D. Tung, W.H. Frey II, Delivery of interferon-beta to the monkey nervous system following intranasal administration, *Neuroscience (San Diego, CA, U. S.)* 152 (2008) 785–797. <https://doi.org/10.1016/j.neuroscience.2008.01.013>.
- [66] D.B. Renner, A.L. Svitakm, N.J. Gallus, M.E. Ericson, W.H. Frey II, L.R. Hanson, Intranasal delivery of insulin via the olfactory nerve pathway, *J. Pharm. Pharmacol.* 64 (2012) 1709–1714. <https://doi.org/10.1111/j.2042-7158.2012.01555.x>.
- [67] N.L. Johnson, L.R. Hanson, W.H. Frey II, Trigeminal pathways deliver a low molecular weight drug from the nose to the brain and orofacial structures, *Mol. Pharm.* 7 (2010) 884–893. <https://doi.org/10.1021/mp100029t>.
- [68] X. Feng, J. Guo, H.C. Sigmon, R.P. Sloan, A.M. Brickman, F.A. Provenzano, S.A. Small, Brain regions vulnerable and resistant to aging without Alzheimer's disease, *PLoS One* 15 (7) (2020) e0234255. <https://doi.org/10.1371/journal.pone.0234255>.